Published in final edited form as:
Biochem J. 2013 September 1; 454(2): 209–216. doi:10.1042/BJ20130574.

Picking sides: Distinct roles for CYP76M6 and -8 in rice oryzalexin biosynthesis

Yisheng Wu[1], **Qiang Wang**[1], **Matthew L. Hillwig**[1], and **Reuben J. Peters**[2]
Department of Biochemistry, Biophysics, and Molecular Biology, Iowa State University, Ames, IA 50011, USA

Abstract

Natural products biosynthesis often requires the action of multiple cytochromes P450 (CYPs), whose ability to introduce oxygen, increasing solubility, is critical for imparting biological activity. In previous investigations of rice diterpenoid biosynthesis, we have characterized CYPs that catalyze alternative hydroxylation of *ent*-sandaracopimaradiene, the precursor to the rice oryzalexin antibiotic phytoalexins. In particular, CYP76M5, -6 and -8 were all shown to carry out C7β-hydroxylation, while CYP701A8 catalyzes C3α-hydroxylation, with oxy groups found at both positions in oryzalexins A–D, suggesting that these may act consecutively in oryzalexin biosynthesis. Here we report that, although CYP701A8 only poorly reacts with 7β-hydroxy-*ent*-sandaracopimaradiene, CYP76M6 and -8 readily react with 3α-hydroxy-*ent*-sandaracopimaradiene. Notably, their activity yields distinct products, resulting from hydroxylation at C9β by CYP76M6 or C7β by CYP76M8, on different sides of the core tricyclic ring structure. Thus, CYP76M6 and -8 have distinct, non-redundant roles in orzyalexin biosynthesis. Moreover, the resulting 3α,7β- and 3α,9β- diols correspond to oryzalexins D and E, respectively. Accordingly, our results complete the functional identification of the biosynthetic pathway underlying the production of these bioactive phytoalexins. In addition, the altered regiochemistry catalyzed by CYP76M6 following C3α-hydroxylation has some implications for its active site configuration, offering further molecular insight.

Keywords

Diterpenoid; cytochromes P450; enzyme specificity; phytoalexin

INTRODUCTION

CYPs (EC 1.14.13.x) serve important roles in not only xenobiotic metabolism/detoxification, but also natural products biosynthesis. In particular, these heme-thiolate monooxygenases are often responsible for the insertion of oxygen into unreactive carbon-hydrogen bonds of hydrophobic intermediates. The resulting hydroxyl groups then serve to both increase solubility and provide hydrogen-bonding potential that increases the specificity (i.e., binding) of the resulting natural product to its molecular target. Often multiple CYP are required for the production of bioactive natural compounds and, given

[2]Address correspondence to: Reuben J. Peters, Iowa State University, Molecular Biology Building, Rm. 4216, Ames, IA 50011, FAX: (515) 294-0453, rjpeters@iastate.edu.
[1]Current addresses: Conagen Inc., St. Louis, MO (Y.W.); Dept. Plant Physiology, Sichuan Agricultural University, Chengdu, China (Q.W.); Dept. Chemistry, University of Pittsburgh, Pittsburgh, PA (M.L.H.).

AUTHOR CONTRIBUTIONS
The work described here was largely carried out by Y.W., building on preliminary results obtained by Q.W., while M.L.H. provided advice and carried out the described NMR structural analysis, all of which was under the guidance of R.J.P.

their sometimes broad-substrate specificity, it can be difficult to determine if there is defined or preferred order of reactions, and what effect initial hydroxylation reactions may have on subsequently catalyzed reactions. In addition, the homology among CYP paralogs, which can be easily inferred from their grouping into related numbered families and even more closely related lettered sub-families, and that often exhibit similar biochemical activity, further complicates such analysis, and raises the potential of redundancy – e.g., in plants [1].

Plants produce a vast array of natural products that serve various ecological roles, such as in defense against microbial pathogens. In many cases, the biosynthesis of these compounds is induced by infection with the microbial pathogens against which they exhibit antibiotic activity, leading to their designation as phytoalexins [2]. In the important cereal crop plant rice (*Oryza sativa*), these phytoalexins are largely members of the labdane-related diterpenoid (LRD) super-family [3].

LRD biosynthesis is characterized by its initiation via sequential cyclization reactions [4]. First, (bi)cyclization of the general diterpenoid precursor (*E,E,E*)-geranylgeranyl diphosphate (GGPP), generally to the eponymous labdadienyl/copalyl diphosphate (CPP), catalyzed by class II diterpene cyclases (EC 5.5.1.x) then termed CPP synthases (CPSs). This is followed by further cyclization, generally to an olefin, catalyzed by class I (di)terpene synthases (EC 4.2.3.x) often termed *ent*-kaurene synthase-like (KSL) for their derivation from the ancestral enzymatic family member found in all plants for gibberellin phytohormone metabolism. The multicyclic olefins resulting from these initial cyclization reactions are quite hydrophobic – e.g., their partition coefficient (logP) is generally ≥ 8.5. Accordingly, these are invariably further transformed by the addition of oxygen, generally catalyzed by CYPs, to increase their solubility, enabling exertion of biological activity. For example, it has been shown that gibberellin biosynthesis depends on *ent*-kaurene oxidases from the CYP701A sub-family and subsequently acting *ent*-kaurenoic acid oxidases from the CYP88A sub-family [5, 6]. Similarly, conifer resin acid biosynthesis is dependent on CYP720B sub-family members that act on LRD precursors [7, 8].

In the course of functionally characterizing the rice CPS and KSL, we found that consecutively acting OsCPS and OsKSL are close together in the rice genome, along with CYPs [9, 10]. Functional characterization of these CYPs revealed their ability to oxygenate diterpene olefins produced by the co-clustered OsCPS and OsKSL [11-13], as well as those resulting from the action of OsKSL found elsewhere in the rice genome [14], with oxy groups found at the targeted positions in the derived natural products. In addition, similar activity has been demonstrated for CYP701A8, a paralog of the *ent*-kaurene oxidase required for gibberellin metabolism, that also is found elsewhere in the rice genome [15].

Given the alternative positions targeted by the functionally characterized CYP, it is unclear how even diols, which seems to be the minimal degree of modification required to form bioactive LRDs, are generated. For example, while previous isolation of 3α-hydroxy-*ent*-sandaracopimaradiene and re-feeding in rice plant cell-free assays indicated its intermediacy in oryzalexin D and E biosynthesis [16], and we have characterized CYP that will catalyze such C3α (CYP701A8), as well as C7β (CYP76M5, -6, and -8), hydroxylation of the olefin precursor *ent*-sandaracopimaradiene, their ability to act consecutively remains uncertain (Figure 1). Moreover, the known CYP catalyzed reactions are insufficient to generate the observed range of LRDs – e.g., formation of orzyalexin E requires hydroxylation at carbon-9 (C9), but no CYP catalyzing such a reaction with *ent*-sandaracopimaradiene has been found.

Here we provide evidence indicating that oryzalexins D and E are generated by initial C3α-hydroxylation catalyzed by CYP701A8, which alters the subsequent reaction catalyzed by

CYP76M6, such that it hydroxylates C9β instead of C7β, generating oryzalexin E (i.e., the 3α,9β-diol), while CYP76M8 continues to hydroxylate C7β, generating oryzalexin D instead (i.e., the 3α,7β-diol). In addition, we examine the implications of the observed change in regiochemistry for configuration of the CYP76M6 active site.

EXPERIMENTAL

General

Unless otherwise noted, chemicals were purchased from Fisher Scientific (Loughborough, Leicestershire, UK), and molecular biology reagents from Invitrogen (Carlsbad, CA, USA). The logP values presented here were obtained from the SciFinder database (American Chemical Society, Columbus, OH). Gas chromatography (GC) was performed with a Varian (Palo Alto, CA) 3900 GC with Saturn 2100 ion trap mass spectrometer (MS) in electron ionization (70 eV) mode for GC-MS analyses, or with an Agilent 6890N GC with flame ionization detection (FID) for GC-FID analyses. Samples (1 μL) were injected in splitless mode at 50 °C and, after holding for 3 min. at 50 °C, the oven temperature was raised at a rate of 14 °C/min. to 300 °C, where it was held for an additional 3 min. MS data from 90 to 600 *m/z* were collected starting 12 min. after injection until the end of the run.

Recombinant constructs

The CYP701A8, and CYP76M5-8 genes used here are the synthetic, fully codon-optimized and N-terminally modified constructs described previously [14, 15]. However, to optimize metabolic flux, a new CYP expression vector was created by insertion of a DEST cassette into the first multiple cloning site (MCS) of pETDuet (Novagen, Madison, WI), using the NcoI and NotI restriction sites, much as we have described before [17]. To enable dual CYP expression, CYP701A8 was inserted into the second MCS of pETDuet/DEST using the NdeI and XhoI restriction sites, creating a pETDuet/DEST/CYP701A8 vector. Alternatively, CYP76M6 or CYP76M8 were inserted into the second MCS of pETDuet/DEST using the NdeI and XhoI restriction sites. In all three of these cases, a rice CYP reductase (OsCPR1) was inserted via directional recombination into the DEST cassette, creating pETDuet/DEST::OsCPR1/CYP(701A8, 76M6 or -8) constructs, to enable co-expression for feeding studies. CYP76M5-8 were transferred into the pETDuet/DEST/CYP701A8 vector for recombinant expression via directional recombination into the DEST cassette, creating pETDuet/DEST::CYP76M(5-8)/CYP701A8 constructs for balanced CYP expression. To enable co-production of the CYP olefin substrates investigated here, OsKSL7 and OsKSL10 (producing *ent*-cassadiene or *ent*-sandaracopimaradiene, respectively) were inserted via directional recombination into the DEST cassette of the previously described pCDFDuet/DEST/OsCPR1 vector [11], creating pCDFDuet/DEST::OsKSL(7 or 10)/OsCPR1 constructs.

Recombinant expression

All recombinant expression was carried out in the C41 Overexpress strain of *Escherichia coli* (Lucigen, Middleton, WI), using the modular diterpene metabolic engineering concept we have previously described [17], and the vectors described above. Specifically, we co-expressed CYP701A8 with each of CYP76M5-8, using the pETDuet/DEST::CYP76M(x)/CYP701A8 vectors, which were co-transformed with the compatible pGG*e*C, to enable production of the upstream GGPP and, subsequently, *ent*-CPP, as well as the relevant pCDFDuet/ DEST::OsKSL(7 or 10)/OsCPR1 vector, to enable production of the immediate *ent*-cassadiene or *ent*-sandaraco-pimaradiene, respectively, along with the reductase needed for CYP activity. These recombinant strains were grown, typically in 50 mL cultures in TB liquid media at 37 °C to an A_{600} ~ 0.6, shifted to 16 °C for an hour prior to induction with 1 mM IPTG, and supplementation with 5 mg/L riboflavin, and 75 mg/L δ-amino levulinic

acid, then grown for an additional 72 hrs. The resulting diterpenoids were extracted (from the media and cells) with an equal volume of hexane, and analyzed by GC-MS. In every case, the previously reported hydroxylated diterpenoid products were observed, with diols detected in certain cases, as described below.

Diterpenoid production

To obtain the observed dual CYP product in sufficient amounts for NMR analysis, flux was increased into isoprenoid metabolism and the recombinant culture volumes also simply scaled up. To increase flux, the recombinant strain was further transformed with the pMBI vector encoding the bottom half of the mevalonate dependent isoprenoid precursor pathway [18]. This is co-compatible with those mentioned above, and feeding 10 mM mevalonolactone to the resulting recombinant cultures greatly increases (di)terpenoid yield, as previously described [19]. The dihydroxylated diterpenoid was extracted and purified much as previously described [11], using GC-MS to detect the presence of the desired compound (i.e., in various fractions). Briefly, 20 × 1-L cultures were extracted twice with equal volumes of hexanes, and the combined organic extract then dried by rotary evaporation. The resulting residue was dissolved in 10 mL hexanes, which was then extracted thrice with equal volumes of acetonitrile, and the combined acetonitrile extract under a gentle stream of N_2. This was resuspended in 5 mL of hexanes, which was then fractionated via flash chromatography over a 4 g silica column using a Reveleris system (Grace, Deerfield, IL) with UV detection and a hexanes to acetone gradient as the mobile phase. The dihydroxylated diterpenoid eluted in the 20% acetone fraction, which was dried under N_2 and resuspended in 1 mL acetonitrile. Further purification was carried out using an Agilent 1200 series HPLC instrument equipped with autosampler, fraction collector, and diode array UV detection, over a ZORBAX Eclipse XDB-C8 column (4.6 × 150 mm, 5 μm) at a 0.5 mL/min flow rate. The column was pre-equilibrated with 50% acetonitrile/dH_2O, sample loaded, then the column washed with 50% acetonitrile/dH_2O (0-2 min), and eluted with 50%-100% acetonitrile (2-7 min), followed by a 100% acetonitrile wash (7-10 min), leading to purification of a final estimated ~1 mg of the dihyroxylated diterpenoid.

Chemical structure identification

Nuclear magnetic resonance (NMR) spectra were recorded at 25 °C on a Bruker Avance 700 spectrometer equipped with a 5 mm HCN cryogenic probe for ^{1}H and ^{13}C. The purified compound was dried under a gentle stream of N_2, and then dissolved in 0.5 mL deuterated chloroform ($CDCl_3$; Sigma-Aldrich), with this evaporation-resuspension process repeated once more to completely remove the protonated acetonitrile solvent. This sample was placed in NMR microtubes (Shigemi, Allison Park, PA) for analyses, and chemical shifts were referenced using known chloroform-d (^{13}C 77.23, ^{1}H 7.24 ppm) signals offset from TMS. Structural analysis was performed using 1D ^{1}H, and 2D DQF-COSY, HSQC, HMQC, HMBC, and NOESY experiment spectra acquired at 700 MHz, and 1D ^{13}C and DEPT135 spectra (174 MHz) using standard experiments from the Bruker TopSpin v1.4 software. Correlations from the HMBC spectra were used to propose a partial structure, while connections between protonated carbons were obtained from DQF-COSY data to complete the partial structure and assign proton chemical shifts. The structure was further verified using HSQC and DEPT135 to confirm the chemical shift assignments.

Feeding studies

Substrates (*ent*-sandaracopimaradiene, 3α-hydroxy-*ent*-sandaracopimaradiene, and 7β-hydroxy-*ent*-sandaracopimaradiene) were obtained via extraction and purification from metabolically engineered strains of *E. coli*, as previously described [14, 15]. Feeding studies with CYP701A8, CYP76M6 and -8, were then carried out as follows. The CYP were co-expressed with OsCPR1, using the pETDuet/DEST::OsCPR1/CYP (701A8, 76M6, or

76M8) constructs described above, in the C41 Overexpress strain of *E. coli*. These recombinant cultures (50 mL) were supplemented with the addition of 1 mM thiamine, 5 mg/L riboflavin, and 75 mg/L δ-amino levulinic acid at the time of induction, then grown for 24 at 16 °C. The relevant substrates were then fed, to a final concentration of 50 μM (added from 100× stocks in methanol). The cultures were allowed to ferment for an additional 48 hrs, and then extracted with an equal volume of hexanes, following which the resulting products were analyzed by GC-MS. All studies were run in duplicate.

Substrate competition assays

For in vitro assays, cells co-expressing CYP76M6 or -8 with OsCPR1 were harvested 72 h after induction via centrifugation (15 min. at 5,000 × *g*), with the cells then resuspended in 1/10 culture volume of buffer A (0.1 M Tris-HCl, pH 7.2, 20% glycerol, 0.5 mM EDTA) and passed through a French press homogenizer (Emulsiflex-C5; Avestin Inc., Ottawa, Canada) three times at 15,000 psi. The resulting lysates were clarified via centrifugation (15 min. at 15,000 × *g*), and the supernatant used for substrate competition assays. These contained 50 μM 3α-hydroxy-*ent*-sandaracopimaradiene, along with various concentration of *ent*-sandaracopimaradiene, ranging from 5-80 μM, and were carried out in 0.5 mL volumes, containing 100 μL CYP preparation, with reactions initiated by the addition of NADPH (to 0.4 mM). After 10 min. incubations at 30 °C, reactions were terminated by the addition of 50 μL 1M HCl, then extracted thrice with an equal volume of hexanes. In all cases, the enzymatic products were analyzed by GC-MS. The relative specificity constant (k_{cat}/K_M) for *ent*-sandaracopimaradiene versus 3α-hydroxy-*ent*sandaracopimaradiene was calculated from the resulting data, as described [20], with the observed $R^2 > 0.9$ in each case.

Bioinformatic analysis of sub-cellular localization

The potential differential sub-cellular localization of CYP701A8 versus CYP76M6 and -8 was investigated by bioinformatics analysis using four distinct algorithms – CholoroP (http://www.cbs.dtu.dk/services/ChloroP/), Predotar (http://urgi.versailles.inra.fr/predotar/predotar.html), PCLA (http://www.andrewschein.com/cgi-bin/pclr/pclr.cgi), and iPSORT (http://ipsort.hgc.jp/). As controls, the immediately upstream OsKSL7 and -10 were included, as was the CYP701A3 family member previously shown to be in the plastid [21]. The corresponding sequences are CYP76M6 (NP_001047192), CYP76M8 (NP_001047184), CYP701A8 (NP_001057905), CYP701A3 (NP_197962), OsKSL7 (NP_001047186), and OsKSL10 (NP_001066799).

RESULTS

Probing consecutive hydroxylation reactions via metabolic engineering

The potential sequential activity of CYP701A8 with CYP76M5-8 in oryzalexin A-F and/or phytocassane A-E biosynthesis (e.g., Figure 1) was investigated via a synthetic biology approach. In particular, using codon-optimized genes for these CYP to enable functional expression in *E. coli* [14, 15]. Using a previously developed modular metabolic engineering system [17], CYP701A8 was then co-expressed with each of CYP76M5-8, along with the requisite CYP reductase (CPR), and biosynthetic enzymes for production of the corresponding LRD olefin precursor (i.e., either *ent*-cassadiene or *ent*-sandaracopimaradiene). While only trace amounts of any dihydroxylated product were observed, in the course of these initial studies we noted that the amount of hydroxylated product was dependent on which plasmid the relevant CYP was cloned into, with higher yields observed when this was the pET derived pDEST14 vector as opposed to pCDFDuet. Accordingly, we incorporated use of the pETDuet vector to enable expression of dual CYPs, sub-cloning the invariable CYP701A8 into the second MCS and a DEST cassette into the

first MCS to enable modular assembly of constructs for balanced co-expression of CYP701A8 with each of CYP76M5-8.

Using these improved constructs, it was possible to observe reasonable production of both of the expected hydroxylated products from CYP701A8 and any of CYP76M5-8 with either *ent*-cassadiene or *ent*-sandaracopimaradiene in the appropriately engineered *E. coli*. Moreover, although no dihydroxylated products were observed with *ent*-cassadiene, such products were observed with *ent*-sandaracopimaradiene. In particular, resulting from the activity of CYP701A8 with either CYP76M6 or -8 (Figure 2). Notably, despite the fact that CYP76M6 and -8 both catalyze C7β-hydroxylation with *ent*-sandaracopimaradiene [14], the dihydroxylated products were not the same, indicating a change in regiochemistry for one of the hydroxylation reactions. Comparison of these products with an authentic standard of oryzalexin E (a kind gift from Prof. Robert Coates, Univ. Illinois), demonstrated that CYP701A8 and CYP76M6 together produce this 3α,9β-diol, indicating a change in regiochemistry, from C7 to C9, of the CYP76M6 catalyzed hydroxylation reaction following C3α hydroxylation of *ent*-sandaracopimaradiene by CYP701A8.

Identification of CYP701A8 and CYP76M8 product as oryzalexin D

To enable production of sufficient amounts of the unknown dihydroxylated diterpenoid product of CYP701A8 and CYP76M8 acting on *ent*-sandaracopimaradiene for structural analysis by NMR, we increased flux into terpenoid metabolism in the metabolically engineered *E. coli*. Specifically, the endogenous methyl erythritol phosphate isoprenoid precursor supply pathway was supplemented by incorporation of the bottom “half” of the mevalonate dependent pathway, along with feeding of mevalonate, which significantly increases yield, as previously described [19]. This enabled production of approximately a milligram from not unreasonable quantities of recombinant culture (20-L), with the resulting diterpenoid extracted and purified by flash chromatography and HPLC. From the subsequent NMR analysis (Figure 3 and Table 1), it was possible to assign the position of the two hydroxyl groups to C3α and C7β, with the resulting diol then corresponding to the oryzalexin D expected from the originally observed olefin hydroxylation reactions (see Figure 1).

Defining CYP reaction order

While change in CYP76M6 catalytic regiochemistry presumably results from action on 3α-hydroxy-*ent*-sandaracopimaradiene rather than *ent*-sandaracopimaradiene, the order of reactions in oryzalexin D biosynthesis was uncertain. Feeding experiments demonstrated the expected conversion of 3α-hydroxy-*ent*-sandaracopimaradiene to oryzalexin E by CYP76M6. Similarly, CYP76M8 readily converts this to oryzalexin D. By contrast, CYP701A8 only poorly reacts with 7β-hydroxy-*ent*-sandaracopimaradiene, producing only trace amounts of oryzalexin D (Figure 4).

The increased solubility of 3α-hydroxy-*ent*-sandaracopimaradiene relative to *ent*sandaracopimaradiene complicated comparison of the kinetic constants obtained in reactions with these as substrates. Thus, we turned to direct comparison in substrate competition assays [20]. In particular, running reactions with the CYP76M6 and -8 that are active with both, in the presence of a constant amount of 3α-hydroxy-*ent*-sandaracopimaradiene (50 μM) and varying levels of *ent*-sandaracopimaradiene. These studies revealed that CYP76M6 exhibits a clear preference for 3α-hydroxy-*ent*-sandaracopimaradiene versus *ent*-sandaracopimaradiene, with a relative catalytic efficiency for *ent*-sandaracopimaradiene relative to 3α-hydroxy-*ent*-sandaracopimaradiene of 0.03 (i.e., ~33-fold increase in k_{cat}/K_M). By contrast, CYP76M8 seems to exhibit a slight preference

for *ent*-sandaracopimaradiene, with a relative catalytic efficiency of 3.3 for this versus 3α-hydroxy-*ent*-sandaracopimaradiene.

While this kinetic analysis leaves some uncertainty in preferred reaction order, at least for biosynthesis of the 3α,7β-diol, 3α-hydroxy-*ent*-sandaracopimaradiene is readily detectable in planta [15], while 7β-hydroxy-*ent*-sandaracopimaradiene was not previously detected [14]. Here, through pre-fractionation, we were able to detect 7β-hydroxy-*ent*-sandaracopimaradiene, but it is only present at ~1% of the amount of 3α-hydroxy-*ent*-sandaracopimaradiene. These results then indicate that oryzalexin biosynthesis proceeds via initial hydroxylation of *ent*-sandaracopimaradiene by CYP701A8 at the C3α position, followed by alternative hydroxylation reactions catalyzed by CYP76M6 or -8 at the C9β or C7β positions, producing oryzalexins E and D, respectively (Figure 5).

Plant di-, as well as mono-, terpenoid biosynthesis is initiated in plastids, while CYP are almost invariably localized to the endoplasmic reticulum [22]. For example, the limonene (monoterpene) hydroxylases (CYP71B sub-family members) from *Mentha* species [23], and the CYP720B sub-family members involved in conifer diterpenoid resin acid biosynthesis [24]. However, it has been previously reported that the CYP701A3, the *ent*-kaurene oxidase required for gibberellin phytohormone biosynthesis in *Arabidopsis thaliana* [25, 26], is localized on the plastid membrane, providing it ready access to its *ent*-kaurene substrate [21]. Hypothesizing that similar plastid localization and increased substrate access for the rice CYP701A8 might help explain the observed higher levels of 3α-hydroxy-*ent*-sandaracopimaradiene relative to 7β-hydroxy-*ent*-sandaracopimaradiene in planta, we carried out bioinformatics analysis to predict sub-cellular localization. Strikingly, CYP701A8 is predicted to be in the plastid by two of the four utilized algorithms, just as is CYP701A3, while CYP76M6 and -8 are not (Table 2). Given the clear plastid localization of the immediately upstream OsKSL10 (as well as OsKSL7), such co-localization of CYP701A8 may provide preferential access to the diterpene olefins, leading to the observed accumulation of its product, relative to that of CYP76M6 and -8, in planta.

DISCUSSION

The use of CYPs is widespread in natural product biosynthesis, and is especially prevalent with terpenoids, where the production of highly hydrophobic olefin intermediates essentially necessitates the action of these membrane-associated monooxygenases. However, we have relatively limited understanding of how these operate, and it can be particularly opaque how multiple CYPs act in common biosynthetic processes. For example, while gibberellin biosynthesis follows a defined CYP reaction order [5, 6], as does biosynthesis of the sesquiterpenoid lactone costunolide [27], the reaction order for the multiple relevant CYPs is not entirely clear in biosynthesis of the diterpenoid paclitaxel/taxol [28], as well as the triterpenoid glycyrrhizin [29].

While the work reported here directly applies to biosynthesis of the rice LRDs, which act as phytoalexins and allelochemicals [30, 31], the use of LRDs, at least as phytoalexins, seems to extend beyond rice and be widespread throughout the *Poaceae* plant family [3]. For example, wheat (*Triticum aestivum*) contains expanded CPS and KSL gene families, and the transcription of certain members is induced by at least UV-irradiation, with the encoded enzymes further exhibiting biochemically diverse function [32-34], much like that of the rice homologs involved in phytoalexin biosynthesis [3]. Moreover, maize (*Zea mays*) not only has been found to contain at least a CPS whose transcription is induced by fungal infection [35], but also more directly demonstrated to produce LRD phytoalexins – i.e., kauralexins A1-3 and B1-3, which exhibit anti-fungal activity [36]. Thus, understanding LRD biosynthesis has broader importance.

Although oxygens can be incorporated during the reactions catalyzed by either class II diterpene cyclases [37-40], and/or class I diterpene synthases [41-47], LRD biosynthesis generally proceeds through a diterpene olefin intermediate [4]. These are strongly hydrophobic (logP ≥ 8.5), requiring the incorporation of oxygen to increase polarity and solubility. Moreover, while addition of a single oxygen does increase solubility, the resulting compounds resemble cholesterol (e.g., 3α-hydroxy-*ent*-sandaracopimaradiene), and are then expected to still partition into membranes. Hence, it perhaps is not surprising that the bioactive rice LRDs contain a minimum of two oxygens, which reduces their logP to ~5 (e.g., 5.0 and 4.9 for oryzalexins D and E, respectively), indicating that these will exhibit significant solubility in natural settings.

Given the invariable use of CYP to introduce these oxygens, investigation of their consecutive action is then critical. Here we not only provide evidence elucidating the biosynthesis of bioactive LRDs, but also demonstrate flux through dual plant CYP mediated steps in bacteria engineered for complete such metabolism, further supporting the utility of this synthetic approach to investigating biosynthetic pathways.

We have hypothesized that phytocassane biosynthesis would proceed via early C3α and C11α hydroxylation [3], which can be catalyzed with the *ent*-cassadiene olefin precursor by CYP701A8, and CYP76M7 and -8, respectively [11, 14, 15]. However, we do not observe production of any dihydroxylated *ent*-cassadiene in cultures co-expressing CYP701A8 and CYP76M7 (or -8), despite the presence of the expected C3α- and C11α-(mono)hydroxylated-*ent*-cassadiene demonstrating that both CYP are active. This suggests that phytocassane biosynthesis may not proceed via this pair of reactions and/or utilizes other enzymes for this purpose.

On the other hand, the production of dihydroxylated *ent*-sandaracopimaradiene products, upon co-expression of CYP701A8 and CYP76M6 or -8, does provide some insight into orzyalexin biosynthesis. Interestingly, this extends beyond the potential roles indicated by their activity with the *ent*-sandaracopimaradiene olefin precursor (Figure 1). In particular, the presence of the C3α-hydroxyl group changes substrate orientation in CYP76M6 such that it targets C9β instead of C7β, which is targeted by both CYP76M6 and -8 with *ent*-sandaracopimaradiene and, in the case of CYP76M8, also with the derived C3α-hydroxylated compound. Accordingly, our results clarify the biosynthesis of not only oryzalexin D (i.e., the originally expected 3α,7β-diol), but that of oryzalexin E (the 3α,9β-diol) as well (Figure 3).

The change in regiochemistry of the CYP76M6 catalyzed reactions prompted us to more closely examine the underlying alteration in substrate orientation. While C7 and C9 are on opposite ‘sides’, the common β position/hydrogen target does fall on same ‘face’ of the middle ‘B’ ring. Examination of 3D models for the alternative substrates highlights the proximity of these positions, indicating that the catalyzed insertion of oxygen occurs via very similar binding modes, with only a slight perturbation in orientation in the CYP76M6 active site imposed by the presence of a C3α-hydroxyl group. We hypothesize that this is mediated via the presence of a polar group in the CYP76M6 active site that either hydrogen bonds to the hydroxyl, leading to reaction at C9, or binds a water molecule that then drives the observed alternative regiospecificity for C7 with *ent*-sandaracopimaradiene (Figure 6).

We suggest here that oryzalexin biosynthesis proceeds via initial C3α hydroxylation. This has been suggested by previous isolation of 3α-hydroxy-*ent*-sandaracopimaradiene and rice plant derived cell-free assays demonstrating its conversion to oryzalexins D and E [16], along with the relative abundance of this intermediate compared to the alternative 7β-hydroxy-*ent*-sandaracopimaradiene in planta reported here. However, while feeding

experiments are consistent with this suggestion, kinetic analysis indicates that such a reaction order is not driven by intrinsic substrate preference, at least in the case of orzyalexin D (3α,7β-diol) biosynthesis. Intriguingly, it has been previously suggested that members of the CYP701A sub-family, which generally act as *ent*-kaurene oxidases in gibberellin phytohormone biosynthesis are localized to plastids [21], where diterpene olefin intermediates are produced [22]. Bioinformatic analysis of CYP701A8 indicates that this is similarly targeted to the plastid, whereas CYP76M6 and -8 are not (Table 2). Thus, we speculate that initial C3α-hydroxylation by CYP701A8 occurs, at least in part, due to preferential access through its co-localization to the plastid, where *ent*-sandaracopimaradiene is initially produced. CYP76M6 and -8 then have only secondary access due to their more typical endoplasmic reticulum localization. Accordingly, these catalyze subsequent, alternative hydroxylations, CYP76M6 at C9β and CYP76M8 at C7β, yielding oryzalexins E (3α,9β-diol) or D (3α,7β-diol), respectively (Figure 5).

In any case, rather the previously suggested redundancy [14], it now appears that CYP76M6 and -8 play separate roles in rice LRD metabolism, particularly orzyalexin biosynthesis, by reacting with distinct sides of the middle 'B' ring in 3α-hydroxy-*ent*-sandaracopimaradiene. Moreover, our results then elucidate the complete biosynthetic pathways leading to these bioactive phytoalexins, adding to the rather few plant natural products for which such knowledge has been accumulated.

Acknowledgments

We thank Meimei Xu for construction of the pETDuet/DEST vector, and Prof. Robert M. Coates (Univ. of Illinois, Urbana-Champaign) for the kind gift of oryzalexin E.

FUNDING

This work was supported by grants from the USDA-NIFA-NRI/AFRI (2008-35318-05027) and NIH (GM086281) to R.J.P.

Abbreviations used

CPP	copalyl diphosphate
CPS	CPP synthase
CYP	cytochrome P450
FID	flame ionization detection
GC	gas chromatography
KSL	kaurene synthase-like
LRD	labdane-related diterpenoid
MCS	multiple cloning site
MS	mass spectrometry

REFERENCES

1. Nelson D, Werck-Reichhart D. A P450-centric view of plant evolution. Plant J. 2011; 66:194–211. [PubMed: 21443632]
2. VanEtten HD, Mansfield JW, Bailey JA, Farmer EE. Two classes of plant antibiotics: phytoalexins versus 'phytoanticipins'. Plant Cell. 1994; 6:1191–1192. [PubMed: 12244269]

3. Peters RJ. Uncovering the complex metabolic network underlying diterpenoid phytoalexin biosynthesis in rice and other cereal crop plants. Phytochemistry. 2006; 67:2307–2317. [PubMed: 16956633]
4. Peters RJ. Two rings in them all: The labdane-related diterpenoids. Nat. Prod. Rep. 2010; 27:1521–1530. [PubMed: 20890488]
5. Hedden P, Thomas SG. Gibberellin biosynthesis and its regulation. Biochem J. 2012; 444:11–25. [PubMed: 22533671]
6. Peters, RJ. Gibberellin phytohormone metabolism.. In: Bach, T.; Rohmer, M., editors. Isoprenoid synthesis in plants and microorganisms: New concepts and experimental approaches. Springer; New York: 2013. p. 233-249.
7. Ro DK, Arimura G, Lau SY, Piers E, Bohlmann J. Loblolly pine abietadienol/abietadienal oxidase PtAO (CYP720B1) is a multifunctional, multisubstrate cytochrome P450 monooxygenase. Proc Natl Acad Sci U S A. 2005; 102:8060–8065. [PubMed: 15911762]
8. Hamberger B, Ohnishi T, Seguin A, Bohlmann J. Evolution of diterpene metabolism: Sitka spruce CYP720B4 catalyzes multiple oxidations in resin acid biosynthesis of conifer defense against insects. Plant Physiology. 2011; 157:1677–1695. [PubMed: 21994349]
9. Prisic S, Xu M, Wilderman PR, Peters RJ. Rice contains two disparate *ent*-copalyl diphosphate synthases with distinct metabolic functions. Plant Physiol. 2004; 136:4228–4236. [PubMed: 15542489]
10. Wilderman PR, Xu M, Jin Y, Coates RM, Peters RJ. Identification of *syn*-pimara-7,15-diene synthase reveals functional clustering of terpene synthases involved in rice phytoalexin/allelochemical biosynthesis. Plant Physiol. 2004; 135:2098–2105. [PubMed: 15299118]
11. Swaminathan S, Morrone D, Wang Q, Fulton DB, Peters RJ. CYP76M7 is an ent-cassadiene C11α-hydroxylase defining a second multifunctional diterpenoid biosynthetic gene cluster in rice. Plant Cell. 2009; 21:3315–3325. [PubMed: 19825834]
12. Wang Q, Hillwig ML, Peters RJ. CYP99A3: Functional identification of a diterpene oxidase from the momilactone biosynthetic gene cluster in rice. Plant J. 2011; 65:87–95. [PubMed: 21175892]
13. Wu Y, Hillwig ML, Wang Q, Peters RJ. Parsing a multifunctional biosynthetic gene cluster from rice: Biochemical characterization of CYP71Z6 & 7. FEBS Lett. 2011; 585:3446–3451. [PubMed: 21985968]
14. Wang Q, Hillwig ML, Okada K, Yamazaki K, Wu Y, Swaminathan S, Yamane H, Peters RJ. Characterization of CYP76M5-8 indicates metabolic plasticity within a plant biosynthetic gene cluster. J. Biol. Chem. 2012; 287:6159–6168. [PubMed: 22215681]
15. Wang Q, Hillwig ML, Wu Y, Peters RJ. CYP701A8: A rice *ent*-kaurene oxidase paralog diverted to more specialized diterpenoid metabolism. Plant Physiol. 2012; 158:1418–1425. [PubMed: 22247270]
16. Kato H, Kodama O, Akatsuka T. Characterization of an inducible P450 hydroxylase involved in the rice diterpene phytoalexin biosynthetic pathway. Arch. Biochem. Biophys. 1995; 316:707–712. [PubMed: 7864625]
17. Cyr A, Wilderman PR, Determan M, Peters RJ. A Modular Approach for Facile Biosynthesis of Labdane-Related Diterpenes. J. Am. Chem. Soc. 2007; 129:6684–6685. [PubMed: 17480080]
18. Martin VJJ, Pitera DJ, Withers ST, Newman JD, Keasling JD. Engineering a mevalonate pathway in *Escherichia coli* for production of terpenoids. Nature biotechnology. 2003; 21:796–802.
19. Morrone D, Lowry L, Determan MK, Hershey DM, Xu M, Peters RJ. Increasing diterpene yield with a modular metabolic engineering system in E. coli: comparison of MEV and MEP isoprenoid precursor pathway engineering. Appl. Microbiol. Biotechnol. 2010; 85:1893–1906. [PubMed: 19777230]
20. Pi N, Leary JA. Determination of enzyme/substrate specificity constants using a multiple substrate ESI-MS assay. Journal of the American Society for Mass Spectrometry. 2004; 15:233–243. [PubMed: 14766290]
21. Helliwell CA, Sullivan JA, Mould RM, Gray JC, Peacock WJ, Dennis ES. A plastid envelope location of *Arabidopsis ent*-kaurene oxidase links the plastid and endoplasmic reticulum steps of the gibberellin biosynthesis pathway. Plant J. 2001; 28:201–208. [PubMed: 11722763]

22. Croteau, R.; Kutchan, TM.; Lewis, NG. Natural products (secondary metabolites).. In: Buchanan, B.; Gruissem, W.; Jones, R., editors. Biochemistry & Molecular Biology of Plants. Am. Soc. Plant Biologists; Rockville, MD, USA: 2000. p. 1250-1318.

23. Turner GW, Croteau R. Organization of monoterpene biosynthesis in Mentha. Immunocytochemical localizations of geranyl diphosphate synthase, limonene-6-hydroxylase, isopiperitenol dehydrogenase, and pulegone reductase. Plant Physiol. 2004; 136:4215–4227. [PubMed: 15542490]

24. Ro DK, Bohlmann J. Diterpene resin acid biosynthesis in loblolly pine (Pinus taeda): functional characterization of abietadiene/levopimaradiene synthase (PtTPS-LAS) cDNA and subcellular targeting of PtTPS-LAS and abietadienol/abietadienal oxidase (PtAO, CYP720B1). Phytochemistry. 2006; 67:1572–1578. [PubMed: 16497345]

25. Helliwell CA, Poole A, Peacock WJ, Dennis ES. *Arabidposis ent*-kaurene oxidase catalyzes three steps of gibberellin biosynthesis. Plant Physiol. 1999; 119:507–510. [PubMed: 9952446]

26. Helliwell CA, Sheldon CC, Olive MR, Walker AR, Zeevaart JA, Peacock WJ, Dennis ES. Cloning of the *Arabidopsis ent*-kaurene oxidase gene GA3. Proc. Natl. Acad. Sci., U.S.A. 1998; 95:9019–9024. [PubMed: 9671797]

27. Ikezawa N, Gopfert JC, Nguyen DT, Kim SU, O'Maille PE, Spring O, Ro DK. Lettuce costunolide synthase (CYP71BL2) and its homolog (CYP71BL1) from sunflower catalyze distinct regio- and stereoselective hydroxylations in sesquiterpene lactone metabolism. J. Biol. Chem. 2011; 286:21601–21611. [PubMed: 21515683]

28. Guerra-Bubb J, Croteau R, Williams RM. The early stages of taxol biosynthesis: an interim report on the synthesis and identification of early pathway metabolites. Nat Prod Rep. 2012; 29:683–696. [PubMed: 22547034]

29. Seki H, Sawai S, Ohyama K, Mizutani M, Ohnishi T, Sudo H, Fukushima EO, Akashi T, Aoki T, Saito K, Muranaka T. Triterpene functional genomics in licorice for identification of CYP72A154 involved in the biosynthesis of glycyrrhizin. Plant Cell. 2011; 23:4112–4123. [PubMed: 22128119]

30. Xu M, Galhano R, Wiemann P, Bueno E, Tiernan M, Wu W, Chung IM, Gershenzon J, Tudzynski B, Sesma A, Peters RJ. Genetic evidence for natural product-mediated plant-plant allelopathy in rice (Oryza sativa). New Phytol. 2012; 193:570–575. [PubMed: 22150231]

31. Toyomasu T, Usui M, Sugawara C, Otomo K, Hirose Y, Miyao A, Hirochika H, Okada K, Shimizu T, Koga J, Hasegawa M, Chuba M, Kawana Y, Kuroda M, Minami E, Mitsuhashi W, Yamane H. Reverse-genetic approach to verify physiological roles of rice phytoalexins: characterization of a knockdown mutant of OsCPS4 phytoalexin biosynthetic gene in rice. Physiologia plantarum. 2013

32. Wu Y, Zhou K, Toyomasu T, Sugawara C, Oku M, Abe S, Usui M, Mitsuhashi W, Chono M, Chandler PM, Peters RJ. Functional characterization of wheat copalyl diphosphate synthases elucidates the early evolution of labdane-related diterpenoid metabolism in the cereals. Phytochemistry. 2012; 84:40–46. [PubMed: 23009878]

33. Zhou K, Xu M, Tiernan MS, Xie Q, Toyomasu T, Sugawara C, Oku M, Usui M, Mitsuhashi W, Chono M, Chandler PM, Peters RJ. Functional characterization of wheat ent-kaurene(-like) synthases indicates continuing evolution of labdane-related diterpenoid metabolism in the cereals. Phytochemistry. 2012; 84:47–55. [PubMed: 23009879]

34. Toyomasu T, Kagahara T, Hirose Y, Usui M, Abe S, Okada K, Koga J, Mitsuhashi W, Yamane H. Cloning and characterization of cDNAs encoding ent-copalyl diphosphate synthases in wheat: insight into the evolution of rice phytoalexin biosynthetic genes. Biosci Biotechnol Biochem. 2009; 73:772–775. [PubMed: 19270400]

35. Harris LJ, Saparno A, Johnston A, Prisic S, Xu M, Allard S, Kathiresan A, Ouellet T, Peters RJ. The maize *An2* gene is induced by *Fusarium* attack and encodes an *ent*-copalyl diphosphate synthase. Plant Mol Biol. 2005; 59:881–894. [PubMed: 16307364]

36. Schmelz EA, Kaplan F, Huffaker A, Dafoe NJ, Vaughan MM, Ni X, Rocca JR, Alborn HT, Teal PE. Identity, regulation, and activity of inducible diterpenoid phytoalexins in maize. Proc. Natl. Acad. Sci. U. S. A. 2011; 108:5455–5460. [PubMed: 21402917]

37. Falara V, Pichersky E, Kanellis AK. A copal-8-ol diphosphate synthase from the angiosperm Cistus creticus subsp. creticus is a putative key enzyme for the formation of pharmacologically

active, oxygen-containing labdane-type diterpenes. Plant Physiol. 2010; 154:301–310. [PubMed: 20595348]

38. Criswell J, Potter K, Shephard F, Beale MB, Peters RJ. A single residue change leads to a hydroxylated product from the class II diterpene cyclization catalyzed by abietadiene synthase. Org. Lett. 2012; 14:5828–5831. [PubMed: 23167845]
39. Gunnewich N, Higashi Y, Feng X, Choi KB, Schmidt J, Kutchan TM. A diterpene synthase from the clary sage Salvia sclarea catalyzes the cyclization of geranylgeranyl diphosphate to (8R)-hydroxy-copalyl diphosphate. Phytochemistry. 2012; 91:93–99. [PubMed: 22959531]
40. Zerbe P, Chiang A, Yuen M, Hamberger B, Draper JA, Britton R, Bohlmann J. Bifunctional cis-abienol synthase from Abies balsamea discovered by transcriptome sequencing and its implications for diterpenoid fragrance production. J. Biol. Chem. 2012; 287:12121–12131. [PubMed: 22337889]
41. Caniard A, Zerbe P, Legrand S, Cohade A, Valot N, Magnard JL, Bohlmann J, Legendre L. Discovery and functional characterization of two diterpene synthases for sclareol biosynthesis in Salvia sclarea (L.) and their relevance for perfume manufacture. BMC Plant Biol. 2012; 12:119. [PubMed: 22834731]
42. Schalk M, Pastore L, Mirata MA, Khim S, Schouwey M, Deguerry F, Pineda V, Rocci L, Daviet L. Towards a Biosynthetic Route to Sclareol and Amber Odorants. J. Am. Chem. Soc. 2012; 134:18900–18903. [PubMed: 23113661]
43. Keeling CI, Madilao LL, Zerbe P, Dullat HK, Bohlmann J. The primary diterpene synthase products of Picea abies levopimaradiene/abietadiene synthase (PaLAS) are epimers of a thermally unstable diterpenol. J. Biol. Chem. 2011; 286:21145–21153. [PubMed: 21518766]
44. Hall DE, Zerbe P, Jancsik S, Quesada AL, Dullat H, Madilao LL, Yuen M, Bohlmann J. Evolution of conifer diterpene synthases: diterpene resin acid biosynthesis in lodgepole pine and jack pine involves monofunctional and bifunctional diterpene synthases. Plant Physiol. 2013; 161:600–616. [PubMed: 23370714]
45. Zerbe P, Hamberger B, Yuen MM, Chiang A, Sandhu HK, Madilao LL, Nguyen A, Hamberger B, Bach SS, Bohlmann J. Gene discovery of modular diterpene metabolism in nonmodel systems. Plant Physiol. 2013; 162:1073–1091. [PubMed: 23613273]
46. Herde M, Gartner K, Kollner TG, Fode B, Boland W, Gershenzon J, Gatz C, Tholl D. Identification and regulation of TPS04/GES, an Arabidopsis geranyllinalool synthase catalyzing the first step in the formation of the insect-induced volatile C16-homoterpene TMTT. Plant Cell. 2008; 20:1152–1168. [PubMed: 18398052]
47. Martin DM, Aubourg S, Schouwey MB, Daviet L, Schalk M, Toub O, Lund ST, Bohlmann J. Functional annotation, genome organization and phylogeny of the grapevine (Vitis vinifera) terpene synthase gene family based on genome assembly, FLcDNA cloning, and enzyme assays. BMC Plant Biol. 2010; 10:226. [PubMed: 20964856]

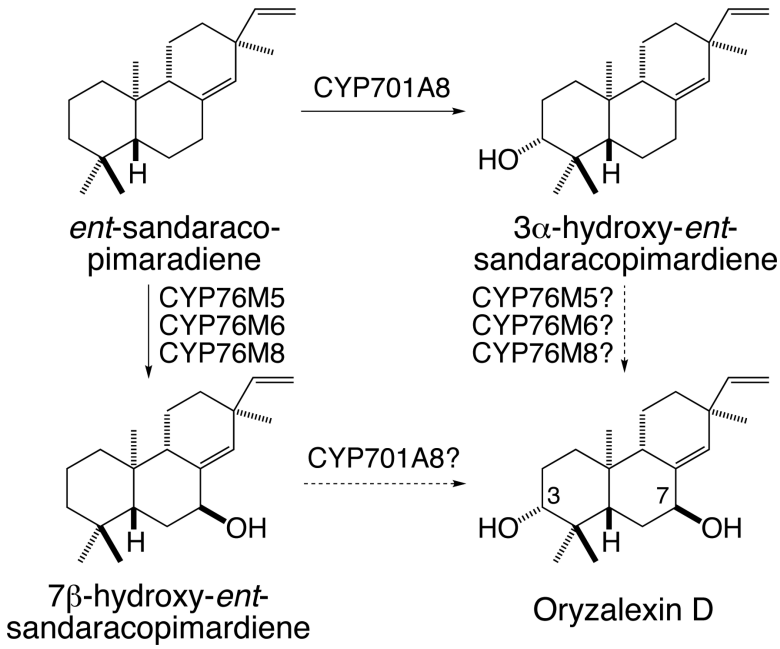

Figure 1.
Previously demonstrated hydroxylation reactions catalyzed by rice CYP with *ent*-sandaracopimaradiene, along with their suggested relevance to orzyalexin D biosynthesis.

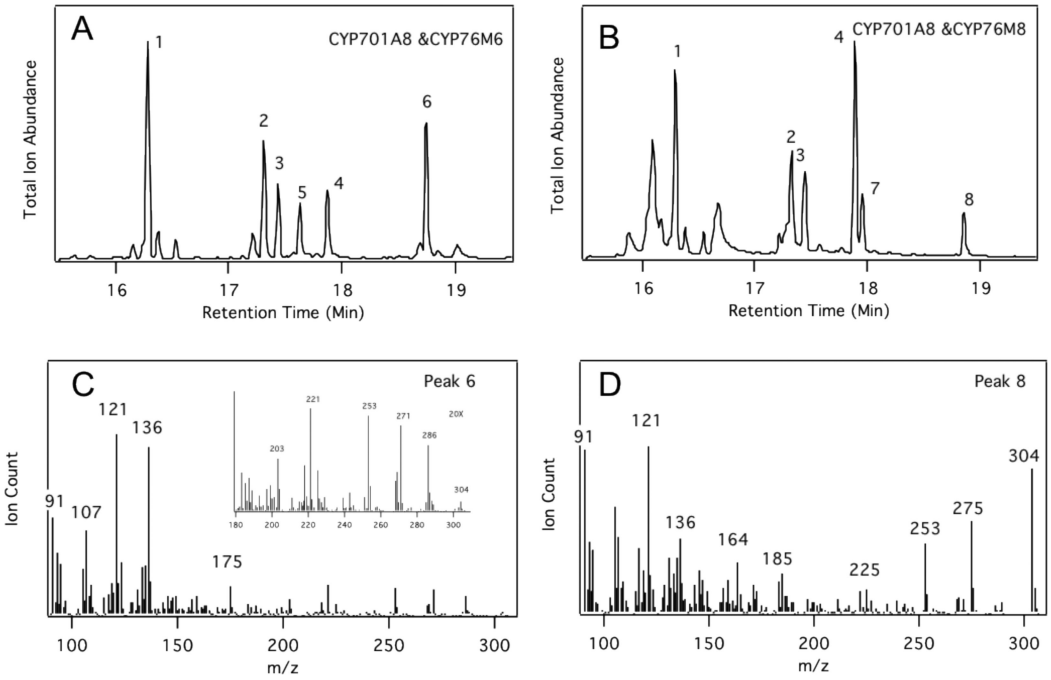

Figure 2.

Dihydroxylation of *ent*-sandaracopimaradiene catalyzed by CYP701A8 and CYP76M6 or -8 as demonstrated by GC-MS. Chromatograms of products resulting from co-expression of CYP701A8 and (A) CYP76M6 or (B) CYP76M8 in *E. coli* engineered to also produce *ent*-sandaracopimaradiene (peak 1, *ent*-sandaracopimaradiene; peak 2, 7β-hydroxy-*ent*sandaracopimaradiene; peak 3, *ent*-copalol; peak 4, 3α-hydroxy-*ent*-sandaracopimaradiene; peak 5, dehydration product of oryzalexin E; peak 6, oryzalexin E; peak 7, dehydration product of oryzalexin D; peak 8, oryzalexin D). Mass spectra of the resulting diols, molecular weight = 304 daltons, from the activity of CYP701A8 and (C) CYP76M6 or (D) CYP76M8.

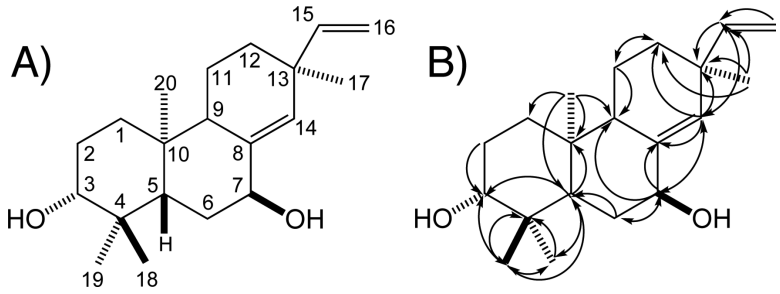

Figure 3.
Structural analysis of oryzalexin D by NMR. (A) numbering. (B) HMBC correlations.

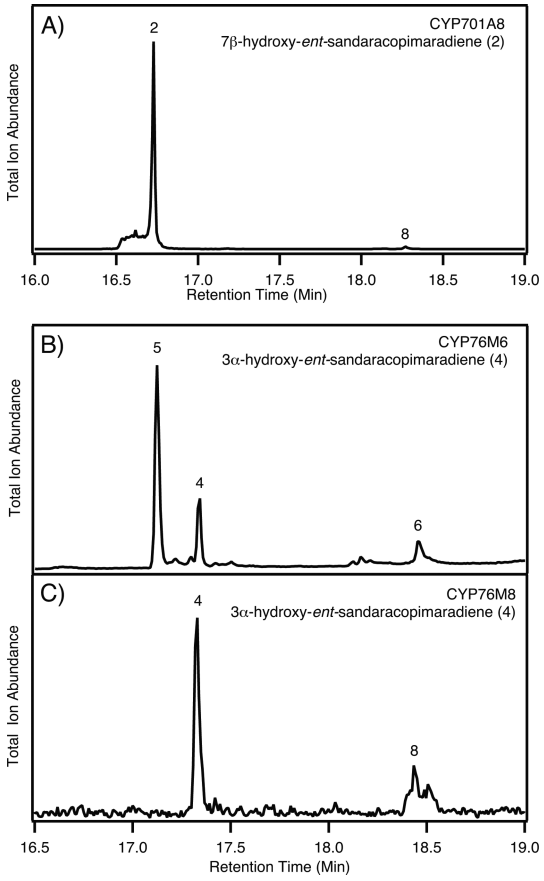

Figure 4.

Substrate feeding indicates reaction order. Chromatograms of products resulting from feeding 3α-hydroxy-*ent*-sandaracopimaradiene to (A) CYP76M6 or (B) CYP76M8, or feeding of 7β-hydroxy-*ent*-sandaracopimaradiene to (C) CYP701A8 (peak numbering as in Figure 2).

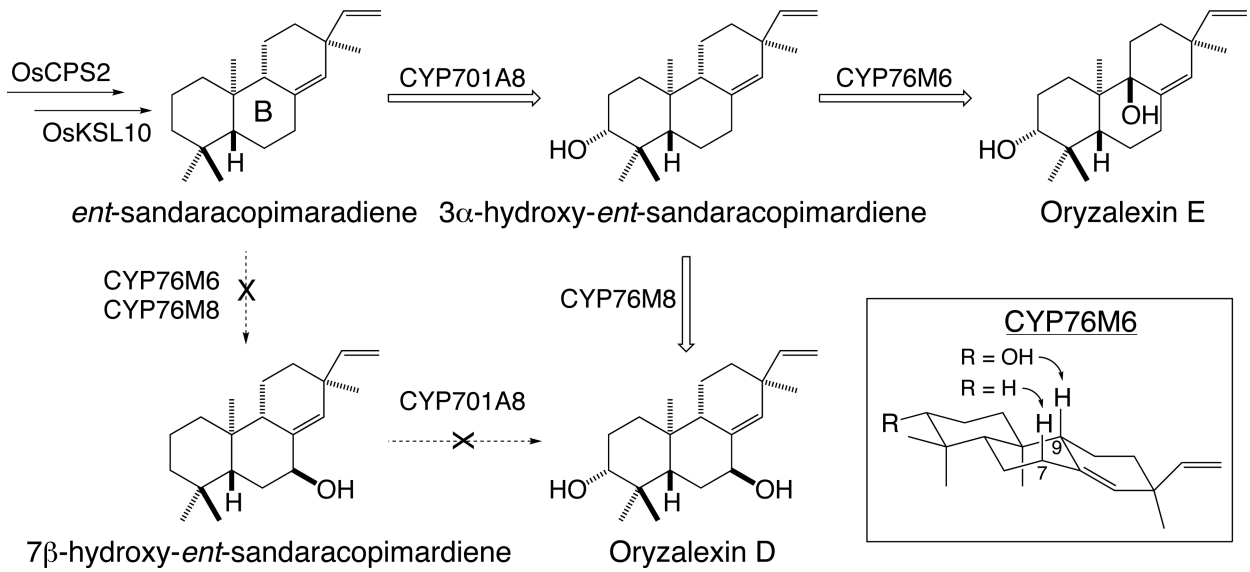

Figure 5.

Proposed biosynthetic pathway for oryzalexins D and E, with indicated roles for CYP701A8 and CYP76M6 and -8, along with observed reactions that do not seem to be relevant in planta. Inset demonstrates the differential reactivity of CYP76M6 (i.e., the effect of 3α-hydroxylation on the catalyzed reaction), with three-dimensional rendering of *ent*-sandaracopimaradiene.

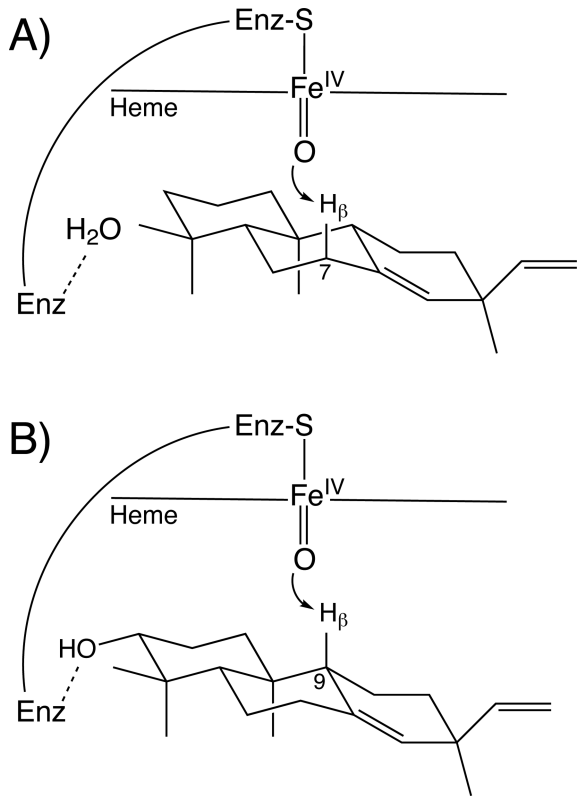

Figure 6.
Schematic for the hypothesized presence of a hydrogen-bonding polar group in the active site of CYP76M6 that imposes the observed change in regiochemistry upon C3α hydroxylation. This binds of water in the presence of (A) *ent*-sandaracopimaradiene or (B) directly to 3α-hydroxy-*ent*-sandaracopimaradiene, dictating the position targeted for hydroxylation by CYP76M6 via the depicted activated ferryl oxo intermediate.

Table 1

^{1}H and ^{13}C NMR assignments for oryzalexin D (3α, 7β-dihydroxy-*ent*-sandaracopimaradiene).

C	δ_C (ppm)	δ_H (ppm), multiplicity	*J* (Hz)
1	37.27	1.212(dt), 1.723(dt)	3.2, 13.2
2	27.77	1.546(m), 1.658(m)	
3	79.10	3.294(dt)	4.8, 11.6
4	38.76		
5	46.60	1.578(m)	
6	29.13	1.589(m), 1.788(m)	
7	73.35	4.203(s-broad)	
8	139.00		
9	46.02	2.073(t)	7.3
10	37.68		
11	18.50	1.476(m), 1.610(m)	
12	34.42	1.369(dt), 1.467(m)	3.1, 12.5
13	38.50		
14	134.90	5.516(s)	
15	148.30	5.765(q)	10.3, 17.5
16	110.99	4.912(d), 4.923(d)	10.3, 17.5
17	25.88	1.030(s)	
18	15.82	0.810(s)	
19	28.00	1.008(s)	
20	14.38	0.761(s)	

Table 2

Plastid prediction results

	ChloroP	Predotar	PCLA	iPSORT
CYP76M6	-	-	-	-
CYP76M8	-	-	-	-
CYP701A8	-	Y	Y	-
CYP701A3	Y	-	Y	-
OsKSL7	Y	Y	Y	Y
OsKSL10	Y	-	Y	Y